Short monolithic dual-wavelength single-longitudinal-mode DBR phosphate fiber laser

Lingyun Xiong,[1,*] Peter Hofmann,[2] Axel Schülzgen,[2]
N. Peyghambarian,[3] and Jacques Albert[1]

[1]Department of Electronics, Carleton University, 1125 Colonel By Drive, Ottawa, Ontario K1S 5B6, Canada

[2]College of Optics and Photonics, CREOL, University of Central Florida, Orlando, Florida 32816, USA

[3]College of Optical Sciences, University of Arizona, Tucson, Arizona 85721, USA

*Corresponding author: lxiong@doe.carleton.ca

We propose and demonstrate a 5-cm-long monolithic dual-wavelength single-longitudinal mode distributed Bragg reflector (DBR) all-phosphate fiber laser. Strong UV-induced fiber Bragg gratings are directly written in highly Er/Yb codoped phosphate fiber. The separation between gratings is selected as 1 cm to only excite two longitudinal modes in the DBR cavity. By exploiting the spatial hole burning effect and the polarization hole burning effect, stable narrow-linewidth dual-wavelength lasing emission with 38 pm wavelength spacing and a total emitted power of 2.8 mW is obtained from this DBR fiber laser. A microwave signal at 4.58 GHz is generated by the heterodyne detection of the dual-wavelength laser.   © 2014 Optical Society of America

OCIS codes: (140.3510) Lasers, fiber; (060.3735) Fiber Bragg gratings; (060.2290) Fiber materials; (060.3738) Fiber Bragg gratings, photosensitivity; (260.5430) Polarization.

http://dx.doi.org/10.1364/AO.53.003848

1. Introduction

Phosphate glass fiber is an important medium for building compact and monolithic optical fiber lasers, as the fiber is capable of hosting higher concentration of erbium and ytterbium ions without causing cluster formation [1]. However, the lack of photosensitivity in phosphate glass fiber often prevented the integration of UV-written intrafiber gratings into the laser cavity. Many phosphate fiber lasers were built by incorporating external reflector mirrors, such as depositing thin film coatings on fiber facets or fusion splicing with conventional silica-based fiber Bragg gratings (FBGs) [2–7]. For these hybrid phosphate-silica glass devices, optical losses and mechanical instabilities at the splicing points present inherent challenges due to the different thermal properties of the two glass types. Recently, we have successfully written strong and thermally stable Bragg gratings directly in phosphate glass fibers using an ArF excimer laser [8,9], and we have demonstrated compact and monolithic cladding-pumped distributed feedback (DFB) lasers in Er/Yb codoped phosphate fiber [10–12]. In [11], a spectrally narrow dual-wavelength laser emission is obtained by cascading two DFB phosphate fiber lasers with pump light propagating in the cladding of the laser chain. In this paper, we demonstrate a dual-wavelength emission from one short monolithic core-pumped distributed Bragg reflector (DBR) phosphate fiber laser. However, because erbium-doped fiber is a homogenously broadened gain medium, the severe mode competition imposes a challenge to achieve simultaneous multiple wavelength oscillation. To establish stable dual-wavelength lasing at room temperature, various techniques have been employed to reduce the mode competition. These include exploiting the spatial

hole burning effect in a linear cavity [13,14], utilizing two spatially separated phase-shifted DFB structures [15,16], exploiting the polarization hole burning effect by using polarization-maintaining FBGs [17–20], inserting a piece of unpumped erbium-doped fiber as a saturable absorber [21,22] and even incorporating a semiconductor optical amplifier as an inhomogenously broadened gain medium [23–26].

In this paper, a 5-cm-long DBR cavity is formed by directly inscribing a pair of 2-cm-long uniform FBGs into Er/Yb codoped phosphate fiber as briefly reported in a short conference paper [27]. Here we present detailed results and analysis about the DBR fiber laser fabrication and optical properties. This complete analysis helps to fully explain the underlying mechanism of the stable dual-wavelength lasing operation of the proposed fiber laser. The 1-cm-long separation between FBGs ensures that only two Fabry–Perot (FP) transmission resonances exist within the grating bandwidth. Therefore, only two longitudinal modes are oscillating in the laser cavity. A polarization analysis of the laser output shows that the two lasing modes belong to different linear polarization states owing to the UV-induced birefringence from the grating inscription. Hence, stable dual-wavelength emission with 38 pm wavelength spacing is achieved by exploiting the spatial hole burning effect and the polarization hole burning effect to reduce mode competition. The characterization on the states of polarization of the dual-wavelength laser output, along microscopic images of the UV-induced surface damages on the phosphate glass fiber, suggests that the stable dual-wavelength lasing operation can be mainly attributed to the polarization hole burning effect. Compared with other dual-wavelength fiber lasers, the proposed DBR fiber laser has the advantages of simple structure, effective cost, and ease of fabrication. Without using polarization maintaining fiber, the small UV-induced birefringence in the doped fiber is sufficient to achieve the stable dual-wavelength emission. The slope efficiency of the proposed dual-wavelength phosphate fiber laser is low. This is mainly because of the relatively low UV photosensitivity of phosphate fibers (compared to silica fibers), which prevents the achievement of high reflectivity gratings with optimized refractive index modulation along the fiber axis as well as because of the large splice losses between the phosphate fiber and SMF-28 fiber. However, achieving a high slope efficiency is not the absolute requirement for most applications of this type of laser [19,21,26].

2. Experimental Setup

Configuration of the proposed short dual-wavelength DBR phosphate fiber laser is shown in Fig. 1. A 980 nm laser diode delivers up to 500 mW pump light to the doped phosphate fiber through a 980/1550 nm wavelength division multiplexer (WDM). We measure the laser signal in the same direction as the pump light propagation in this codirectional
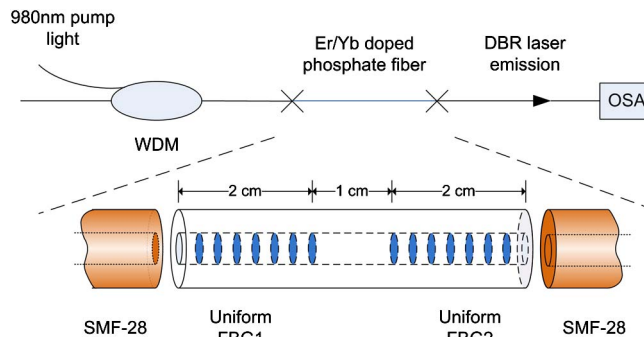

Fig. 1. Schematic of the short dual-wavelength single-longitudinal mode DBR phosphate fiber laser.

pump configuration. The whole DBR laser cavity is fabricated on a 5-cm-long Er/Yb co-doped phosphate fiber, whose core is doped with 1 wt.% Er_2O_3 and 2 wt.% Yb_2O_3. The phosphate fiber was fusion spliced to standard telecommunications fiber pigtails (Corning SMF-28) for compatible use with other devices. Intracore Bragg gratings were directly written in the phosphate glass fiber using a phase mask irradiated by intense UV radiation from a pulsed 193 nm ArF excimer laser. As shown in Fig. 1, two uniform FBGs (FBG1 and FBG2), each 2 cm long, were inscribed on each side of the phosphate fiber individually. The unexposed separation between them is 1 cm long. During grating fabrication, FBG1 was first written with a 2-cm-long phase mask, and then FBG2 was written with the same phase mask after the fiber had been manually translated to its desired position. To keep the resonance peaks of the gratings matched, the same tension was applied on the phosphate fiber during the fabrication of both gratings. The reflectivities of FBG1 and FBG2 are 95% and 90%, and the lower reflectivity FBG2 is used as the output coupler of the laser.

3. Experimental Results and Discussion

The spectral characteristics of the DBR gratings were measured with an optical spectrum analyzer (OSA). Figure 2 illustrates the transmission spectra of a single-grating FBG1 and of the dual-grating DBR structure written in the doped phosphate fiber. The Bragg resonances of the gratings FBG1 and FBG2 are at 1531.25 nm. The FP transmission maxima are not clearly observed in the grating rejection band, mainly because the narrow bandwidths of FP transmission peaks are beyond the resolution limit (0.01 nm) of the OSA and also because of losses within the FP cavity when the fiber is not pumped [28]. For this FP cavity, the theoretical wavelength spacing between the transmission resonance peaks is calculated to be 38 pm according to the formula given in [29]. Therefore, only two FP resonances can oscillate within the about 100 pm 3 dB bandwidth of the FBGs.

The fabricated DBR cavity is then employed to build the monolithic dual-wavelength phosphate fiber laser, according to the schematic shown in Fig. 1.
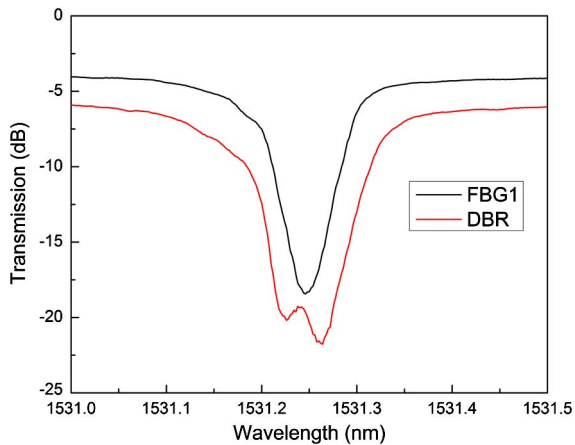
Fig. 2. Transmission spectra of the uniform FBG1 and the DBR grating structure in the Er/Yb-doped phosphate fiber.

As the heavily doped fiber generates the excessive heat upon high pump power, in this forward pump configuration, FBG1 will experience a larger heat-induced redshift in wavelength than FBG2. This wavelength mismatch poses a potential difficulty in achieving laser oscillation. To avoid the heat-induced wavelength mismatch between FBG1 and FBG2, a passive cooling scheme is used by mounting the doped fiber on a metal plate.

Figure 3 illustrates the optical spectra of the DBR phosphate fiber laser at launched pump powers of 350 and 500 mW, respectively. We should note that the real launched pump powers into the doped phosphate fiber are only 223 and 319 mW because of the large total splice losses between 980 nm laser diode pigtail and the doped phosphate fiber. Dual-wavelength lasing at the designed Bragg wavelength is observed, and the optical signal to noise ratio is about 60 dB. The linewidths of each lasing peak are too narrow to be resolved by the OSA. The wavelength spacing of the two lasing peaks is 38 pm, which agrees with the theoretical longitudinal mode spacing of this DBR structure. The output powers at the two laser emission peaks are nearly equal at a
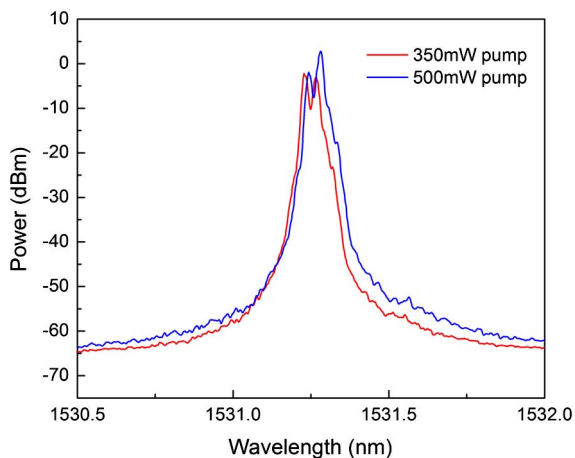
pump power of 350 mW, but when the pump power is increased to 500 mW, the long wavelength lasing peak is favored. This suggests that the cavity loss of the two longitudinal lasing modes is pump power dependent. We note that, although the laser cavity is passively cooled by mounting the fiber on a metal plate, during laser operation the transmission spectra of our DBR structure changes slightly as a result of pump induced residual temperature variations.

In order to investigate long-term stability of the laser output, the optical spectra of the dual-wavelength fiber laser pumped at 500 mW are measured at time intervals of 1 min, as shown in Fig. 4(a). The laser spectrum is stable over the
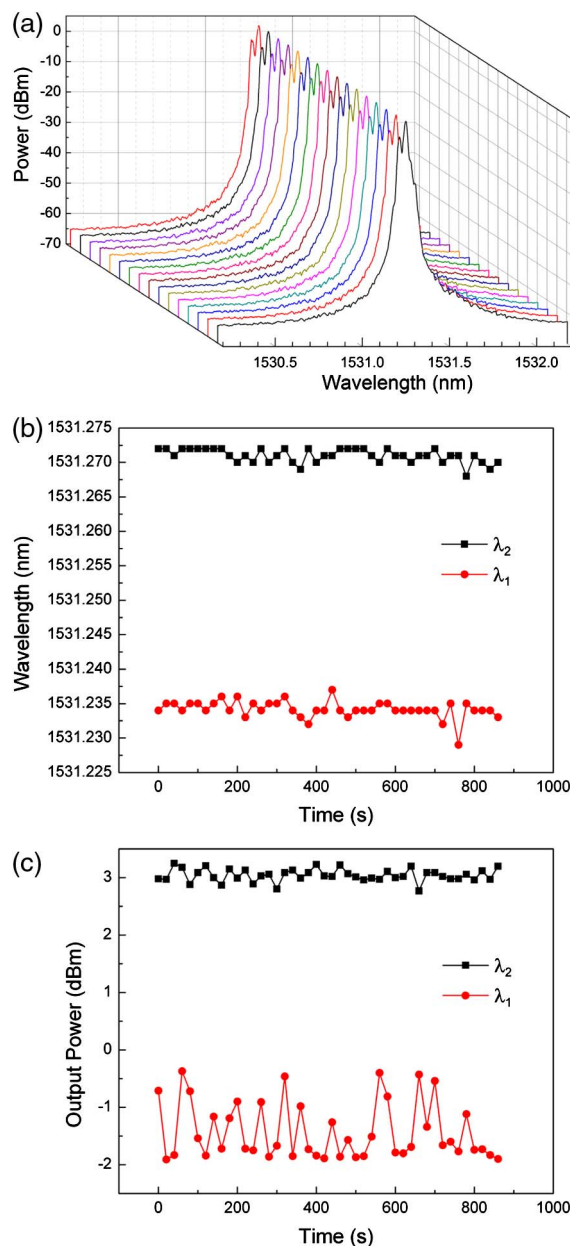

Fig. 4. (a) Laser output spectra for 16 continuous sweeps taken at 1 min intervals; fluctuation of (b) wavelengths and (c) peak output powers for dual-wavelength laser pumped at 500 mW.

Fig. 3. Optical spectra of the dual-wavelength DBR phosphate fiber laser pumped at 350 and 500 mW.

observation period. The stabilities of output power and lasing wavelength of the two lasing peaks are plotted in Figs. 4(b) and 4(c). As shown in the figures, both lasing wavelengths are stable with variations of less than 10 pm, which is the resolution limit of the OSA. The peak output powers at each lasing wavelength exhibit different fluctuations: the strong lasing peak with an output power of 2.98 dBm (1.99 mW) varies by 0.48 dB over the observation period. In contrast, a larger relative power variation of up to 1.53 dB is observed for the weak lasing peak with an output power of −1.16 dBm (0.77 mW). In absolute terms, the peak output powers fluctuate at both emission wavelengths by ±0.1 mW. The laser performance is stable over a long-term period. One additional measurement was taken after 1 h of the laser continuously running, showing consistent wavelength and output power with those measured during the first 15 min. It appears difficult at this time to increase the slope efficiency of this structure beyond about 1%, as achieved here, because of the combination of constraints that come into play simultaneously: basically the limited maximum index modulation of this photosensitive process makes it difficult to achieve laser cavity mirrors with high reflectivity and sufficient bandwidth to cover the two lasing wavelengths. The index modulations of FBG1 and FBG2 are 7.1×10^{-5} and 5.8×10^{-5}, respectively. A further improvement of index modulation can be accomplished by increasing the pulse fluence of the UV laser used for grating fabrication or employing a thermal growth process by heating gratings at high temperatures, which is a unique feature for phosphate FBGs [8,9]. Fortunately, high slope efficiency is not an absolute requirement for this type of laser application.

Figure 5 shows the measured microwave signal generated by photodetecting the dual-wavelength DBR fiber laser. The measurement is performed with an electrical spectrum analyzer (ESA) operating at a resolut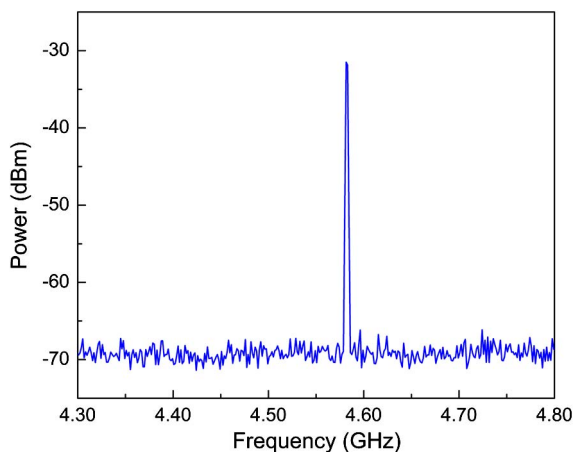ion bandwidth of 3 MHz and a sweep span of 600 MHz. The beating signal has noticeable amplitude fluctuations due to the gain competition of the two lasing peaks, but its frequency is stabilized at 4.58 GHz with a drift of less than 30 MHz. The 3 dB bandwidth of the signal is approximately 4 MHz. No strong microwave signal is found at other frequencies, meaning that both lasing peaks correspond to a single longitudinal mode.

The polarization state of the dual-wavelength laser is characterized with an analyzer and the OSA. The laser output spectra through the analyzer oriented at different angles are shown in Fig. 6. The short- and long-lasing wavelengths are assigned as λ_1 and λ_2. The reference angle (0°) is defined for the angle corresponding to the maximum power for the dominant longitudinal lasing mode (at λ_2). Rotation of the analyzer by 90° minimizes the power of the long wavelength lasing line, but the maximum power output of the short wavelength (λ_1) lasing line occurs at an analyzer angle of 70°. The polarization extinction ratio (PER) is about 20 dB at λ_1 and 10 dB at λ_2. The polarization states of λ_1 and λ_2 are schematically plotted in the inset of Fig. 6. Ideally, the polarization hole burning effect is most effective for orthogonal polarization states, but this does not appear to be the case here. This deviation of the angle between polarization states has been determined to originate from the grating fabrication process. As the FBGs are side-written with UV exposure from one direction, a UV-induced birefringence is introduced for each FBG. Because of the polarization hole burning effect, the UV-induced birefringence favors light to lase along the orthogonal eigen polarization states for FBGs. The origin of the 70° rotation between the two lasing polarizations was verified to come from an accidental rotation of fiber by the same angle during the manual translation of the fiber between the fabrication of FBG1 and FBG2. This is confirmed by the following observation. Figure 7 shows microscope images of the cladding surface on the ends of the

Fig. 5.   Electrical spectrum of the microwave signal generated by the dual-wavelength DBR phosphate fiber laser.
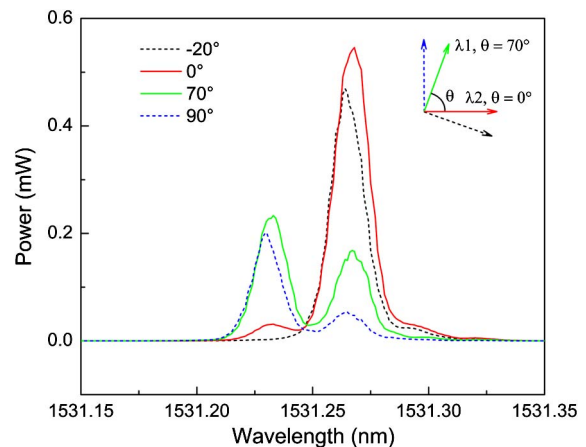

Fig. 6.   Laser output spectra transmitted through a polarization analyzer at different angles. The inset shows the polarization states of two lasing lines (λ_1 and λ_2: short- and long-lasing wavelengths).
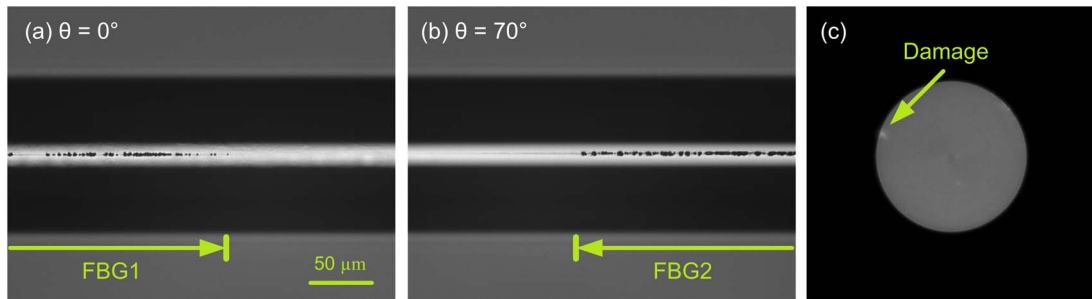
Fig. 7. Microscope images of UV-induced damages on the phosphate fiber cladding surface for (a) FBG1 with rotation angle $\theta = 0°$; (b) FBG2 with rotation angle $\theta = 70°$; (c) cross-section of a cleaved FBG.

UV-induced FBGs. As the phosphate glass is softer than silica glass, an ablation effect readily occurs under intense UV exposure. During the UV inscription of the gratings, small and shallow surface damage [as shown in Fig. 7(c)] is caused on the phosphate fiber outer cladding surface. Carefully rotating the fiber under microscope objective lens, and comparing the orientation angles of the damage for FBG1 and FBG2, the rotation angle between the UV incident directions is found to be about 70°. The above observation confirms that the stable dual-wavelength oscillation in the DBR cavity is mainly owing to a polarization hole burning effect.

4. Conclusion

A 5-cm-long core-pumped monolithic DBR fiber laser is fabricated by directly writing Bragg gratings in highly Er/Yb codoped phosphate fiber. Stable narrow-linewidth dual-wavelength emission with a wavelength spacing of 38 pm and a total emitted power of 2.8 mW is obtained from this DBR fiber laser. A microwave signal at a frequency of 4.58 GHz and stability of 30 MHz is generated by this dual-wavelength fiber laser.

References

1. B. Hwang, S. Jiang, T. Luo, J. Watson, G. Sorbello, and N. Peyghambarian, "Cooperative upconversion and energy transfer of new high Er^{3+}- and Yb^{3+}–Er^{3+}-doped phosphate glasses," J. Opt. Soc. Am. B **17**, 833–839 (2000).
2. C. Spiegelberg, J. Geng, Y. Hu, Y. Kaneda, S. Jiang, and N. Peyghambarian, "Low-noise narrow-linewidth fiber laser at 1550 nm," J. Lightwave Technol. **22**, 57–62 (2004).
3. T. Qiu, S. Suzuki, A. Schülzgen, L. Li, A. Polynkin, V. Temyanko, J. V. Moloney, and N. Peyghambarian, "Generation of watt-level single-longitudinal-mode output from cladding-pumped short fiber lasers," Opt. Lett. **30**, 2748–2750 (2005).
4. L. Li, A. Schülzgen, V. L. Temyanko, M. M. Morrell, S. Sabet, H. Li, J. V. Moloney, and N. Peyghambarian, "Ultracompact cladding-pumped 35-mm-short fiber laser with 4.7-W single-mode output power," Appl. Phys. Lett. **88**, 161106 (2006).
5. A. Schülzgen, L. Li, V. L. Temyanko, S. Suzuki, J. V. Moloney, and N. Peyghambarian, "Single-frequency fiber oscillator with watt-level output power using photonic crystal phosphate glass fiber," Opt. Express **14**, 7087–7092 (2006).
6. X. Zhu, A. Schülzgen, H. Li, L. Li, Q. Wang, S. Suzuki, V. L. Temyanko, J. V. Moloney, and N. Peyghambarian, "Single-transverse-mode output from a fiber laser based on multi-mode interference," Opt. Lett. **33**, 908–910 (2008).
7. S. H. Xu, Z. M. Yang, T. Liu, W. N. Zhang, Z. M. Feng, Q. Y. Zhang, and Z. H. Jiang, "An efficient compact 300 mW narrow-linewidth single frequency fiber laser at 1.5 µm," Opt. Express **18**, 1249–1254 (2010).
8. J. Albert, A. Schülzgen, V. L. Temyanko, S. Honkanen, and N. Peyghambarian, "Strong Bragg gratings in phosphate glass single mode fiber," Appl. Phys. Lett. **89**, 101127 (2006).
9. L. Xiong, P. Hofmann, A. Schülzgen, N. Peyghambarian, and J. Albert, "Photo-thermal growth of unsaturated and saturated Bragg gratings in phosphate glass fibers," in *Bragg Gratings, Photosensitivity, and Poling in Glass Waveguides* (OSA, 2010), paper BTuB1.
10. A. Schülzgen, L. Li, D. Nguyen, C. Spiegelberg, R. M. Rogojan, A. Laronche, J. Albert, and N. Peyghambarian, "Distributed feedback fiber laser pumped by multimode laser diodes," Opt. Lett. **33**, 614–616 (2008).
11. L. Li, A. Schülzgen, X. Zhu, J. V. Moloney, J. Albert, and N. Peyghambarian, "1 W tunable dual-wavelength emission from cascaded distributed feedback fiber lasers," Appl. Phys. Lett. **92**, 051111 (2008).
12. P. Hofmann, A. Pirson-Chavez, A. Schülzgen, L. Xiong, A. Laronche, J. Albert, and N. Peyghambarian, "Low-noise single frequency all phosphate fiber laser," Proc. SPIE **8039**, 803911 (2011).
13. S. Pradhan, G. E. Town, and K. J. Grant, "Dual-wavelength DBR fiber laser," IEEE Photon. Technol. Lett. **18**, 1741–1743 (2006).
14. Y. Yao, X. Chen, Y. Dai, and S. Xie, "Dual-wavelength erbium-doped fiber laser with a simple linear cavity and its application in microwave generation," IEEE Photon. Technol. Lett. **18**, 187–189 (2006).
15. Y. Dai, X. Chen, J. Sun, Y. Yao, and S. Xie, "Dual-wavelength DFB fiber laser based on a chirped structure and the equivalent phase shift method," IEEE Photon. Technol. Lett. **18**, 1964–1966 (2006).
16. G. E. Villanueva, P. Perez-Millan, J. Palaci, J. L. Cruz, M. V. Andres, and J. Marti, "Dual-wavelength DFB erbium-doped fiber laser with tunable wavelength spacing," IEEE Photon. Technol. Lett. **22**, 254–256 (2010).
17. L. Sun, X. Feng, W. Zhang, L. Xiong, Y. Liu, G. Kai, S. Yuan, and X. Dong, "Beating frequency tunable dual-wavelength erbium-doped fiber laser with one fiber Bragg grating," IEEE Photon. Technol. Lett. **16**, 1453–1455 (2004).
18. S. Feng, O. Xu, S. Lu, X. Mao, T. Ning, and S. Jian, "Single-polarization, switchable dual-wavelength erbium-doped fiber laser with two polarization-maintaining fiber Bragg gratings," Opt. Express **16**, 11830–11835 (2008).
19. W. Liu, M. Jiang, D. Chen, S. He, and S. Member, "Dual-wavelength single-longitudinal-mode polarization-maintaining fiber laser and its application in microwave generation," J. Lightwave Technol. **27**, 4455–4459 (2009).

20. P. Rugeland, Z. Yu, O. Tarasenko, G. Tengstrand, and W. Margulis, "Tunable photonic microwave generation based on a novel dual-polarization fiber laser cavity," IEEE Photon. Technol. Lett. **23**, 1878–1880 (2011).
21. X. He, X. Fang, C. Liao, D. N. Wang, and J. Sun, "A tunable and switchable single-longitudinal-mode dual-wavelength fiber laser with a simple linear cavity," Opt. Express **17**, 21773–21781 (2009).
22. B. Lin, S. Chuan Tjin, M. Jiang, and P. Shum, "Tunable microwave generation based on a dual-wavelength fiber laser with an inverse-Gaussian apodized fiber Bragg grating," Appl. Opt. **50**, 4912–4916 (2011).
23. S. Pan, X. Zhao, and C. Lou, "Switchable single-longitudinal-mode dual-wavelength erbium-doped fiber ring laser incorporating a semiconductor optical amplifier," Opt. Lett. **33**, 764–766 (2008).
24. B. Lin, S. C. Tjin, H. Zhang, D. Tang, J. Hao, B. Dong, and S. Liang, "Switchable dual-wavelength single-longitudinal-mode erbium-doped fiber laser using an inverse-Gaussian apodized fiber Bragg grating filter and a low-gain semiconductor optical amplifier," Appl. Opt. **49**, 6855–6860 (2010).
25. M. Tang, H. Minamide, Y. Wang, T. Notake, S. Ohno, and H. Ito, "Tunable Terahertz-wave generation from DAST crystal pumped by a monolithic dual-wavelength fiber laser," Opt. Express **19**, 779–786 (2011).
26. M. A. Ummy, N. Madamopoulos, M. Razani, A. Hossain, and R. Dorsinville, "Switchable dual-wavelength SOA-based fiber laser with continuous tunability over the C-band at room-temperature," Opt. Express **20**, 23367–23373 (2012).
27. L. Xiong, P. Hofmann, A. Schülzgen, N. Peyghambarian, and J. Albert, "A short dual-wavelength DBR phosphate fiber laser," in *CLEO: 2011—Laser Applications to Photonic Applications* (OSA, 2011), paper CTuI3.
28. Y. Liu, L. Wei, and J. W. Y. Lit, "Transmission loss of phase-shifted fiber Bragg gratings in lossy materials: a theoretical and experimental investigation," Appl. Opt. **46**, 6770–6773 (2007).
29. Y. O. Barmenkov, D. Zalvidea, S. Torres-Peiró, J. L. Cruz, and M. V. Andrés, "Effective length of short Fabry–Perot cavity formed by uniform fiber Bragg gratings," Opt. Express **14**, 6394–6399 (2006).